Wang Shuo*, Wei Limin, Cheng Yi and Tan Shuping

Post-weld Heat Treatment and Groove Angles Affect the Mechanical Properties of T92/Super 304H Dissimilar Steel Weld Joints

https://doi.org/10.1515/htmp-2016-0261
Received December 28, 2016; accepted June 11, 2017

Abstract: The microstructures and mechanical properties of dissimilar weld joints between T92 and Super 304H steels were investigated. Dissimilar weld joints with four groove angles were constructed using gas tungsten arc welding. The results showed that post-weld heat treatment improved the mechanical properties of the dissimilar weld joints. The optimal groove angle for T92/Super 304H dissimilar weld joints was found to be 20°, considering mechanical properties. Furthermore, the transformation from equiaxed dendrites to columnar dendrites was observed in the weld metal. Epitaxial growth and delta ferrites were found around the fusion line between the Super 304H and the weld metal.

Keywords: post-weld heat treatment, groove angle, dissimilar steel weld joint, microstructure, mechanical property

Introduction

Dissimilar weld joints are widely used in coal and nuclear power plants. In ultra-supercritical (USC) power plants, the boiler parts that are subjected to lower temperatures are made from ferritic steel for economic reasons. Other parts, operating at higher temperature above 590°C, are built with relatively expensive austenitic heat-resistant steels [1, 2]. Inevitably, there are thousands of dissimilar weld joints between low alloy steels and austenitic heat-resistant steels in modern USC boilers.

***Corresponding author: Wang Shuo,** Material Research Institute, State Key Laboratory of Efficient and Clean Coal-fired Utility Boilers (Harbin Boiler Company Limited), Harbin 150046, Heilongjiang Province, China, E-mail: 57626@163.com
Wei Limin, Cheng Yi, Tan Shuping, Material Research Institute, State Key Laboratory of Efficient and Clean Coal-fired Utility Boilers (Harbin Boiler Company Limited), Harbin 150046, Heilongjiang Province, China

T92 and Super 304H heat-resistant steels were developed by Nippon Steel & Sumitomo Metal. They have been extensively used for super-heaters and re-heaters in USC boilers because of their superior creep strength and excellent resistance to steam oxidation and high-temperature corrosion [3–7]. Much research has been conducted on the mechanical properties and microstructure of T92 [3–9] and Super 304H [10–13]. However, few studies have investigated T92/Super 304H dissimilar weld joints, especially on groove angles. Cao et al. [14, 15] found that the tensile strength of the T92 coarse grain (CG) heat-affected zone (HAZ) decreases owing to its CG tempered martensite structure. They confirmed that the tensile strength of the weld metal was improved by the orientation distribution of grains. Chen et al. [16] investigated the microstructure and mechanical properties of T92/Super 304H dissimilar weld joints after high-temperature aging. Their results showed that the second-phase particles gathered and coarsened along the austenitic grain boundaries. In addition, numerous studies on dissimilar weld joints have been reported for other steel grades [17–26]. Falat et al. [17] revealed that the HAZ of austenitic steel in dissimilar T91/TP316H weld joints was limited to only a narrow region with coarsened polygonal grains. The creep fracture mechanism was thought to be the intergranular dimple tearing by micro-void coalescence at grain boundaries. Shah [26] found that the mechanical properties of Inconel 617 filler materials were much better than Inconel 82 and 310 austenitic stainless steels. Onoro and Dupont [27, 28] reported that the most effective way to avoid delta ferrite in weld metal was to keep the ferrite former elements as low as possible. Denmolaei et al. [18] studied microstructural characterization of dissimilar weld joints between alloy 800 and HP heat-resistant steel. Their results showed that migration of grain boundaries was extensive and epitaxial growth existed at the fusion line.

The aim of the present study is to investigate the mechanical properties and microstructure of T92/Super 304H dissimilar weld joints with different groove angles to find the optimal groove angle range.

Experimental procedure

T92 and Super 304H tubes were joined by gas tungsten arc welding using TP304H as filler metal. Figure 1 shows a schematic diagram of T92/Super 304H dissimilar weld joints. The chemical compositions of the two base metals and the filler metal are given in Table 1. All materials conform to the ASME standards. The welding parameters are shown in Table 2. The welded joints were subjected to post-weld heat treatment (PWHT) at 730–760°C for 2 h to stabilize the austenitic phase and relieve residual stresses.

After X-ray nondestructive testing, specimens were cut, machined and examined to test their mechanical and structural properties. Tensile strength was tested based on NB/T 47014-2011 standard. Microhardness profiles across the weld metal–base metal interface were obtained at a constant load of 187.5 kgF with a loading time of 12 s.

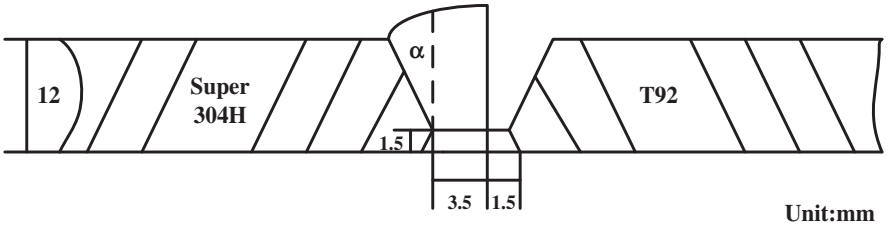

Figure 1: Schematic diagram of T92/Super 304H dissimilar weld joints.

Table 1: Chemical compositions of investigated materials (wt%).

	C	Cr	Mo	V	Nb	Ni	Mn	Si	N	W	Cu
T92	0.11	9.0	0.50	0.23	0.06	0.26	0.46	0.40	0.05	1.64	/
S304H	0.09	18.33	/	/	0.50	8.90	0.80	0.025	0.11	/	2.94
TP304H	0.09	18.5	0.8	/	/	15.9	3.46	.032	/	/	3.00

Table 2: Welding parameters in each welding pass.

Pass	Current (A)	Volt (V)	Welding speed (mm/min)
1	160–200	10–12	1100
2	180–220	11–14	7500
3	200–240	12–14	7400
4	160–180	10–12	7100

Microstructure analysis was conducted by light optical microscopy and scanning electron microscopy equipped with energy X-ray spectroscopy. For light optical microscope and scanning electronic microscope observations, the samples were sanded up to 2000 grit, polished (with diamond paste) and etched.

Results and discussion

Microstructural features

Base metal microstructures

The microstructure of the T92 base metal is displayed in Figure 2(a). It consists of tempered martensite and precipitates along the grain boundaries and in the grains. The precipitates are intergranular MX (M = Nb,V; X = N, C) carbonitrides and $M_{23}C_6$ (M = Fe, Cr) carbides at grain and subgrain boundaries [4, 7, 8]. The microstructure of the Super 304H base metal is shown in Figure 2(b). The microstructure is composed of austenitic grains and precipitates. The average size of austenitic grains is 15 μm. The excellent creep strength of Super 304H was obtained thanks to the precipitates containing $M_{23}C_6$, Cu-rich and MX grains [10, 11, 13].

Weld metal microstructures

Figure 3 shows the microstructures of the weld metal. The equivalent chromium and nickel were calculated by Schaeffer equations [29]. Figure 3(d) shows evidence that TP304H filler had completely austenitized because

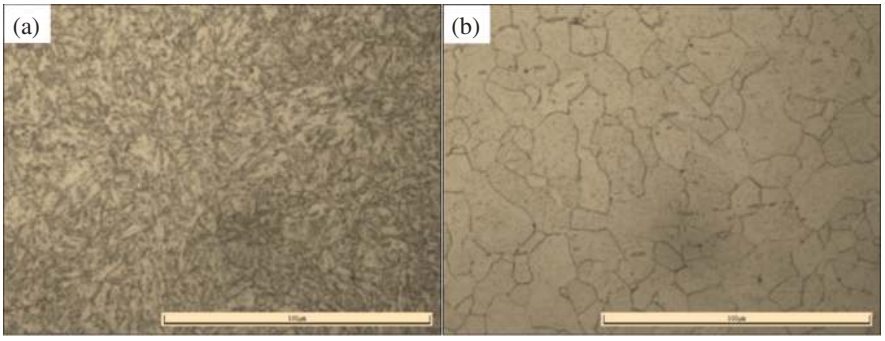

Figure 2: Microstructures of the base materials (a) T92 (b) Super 304H.

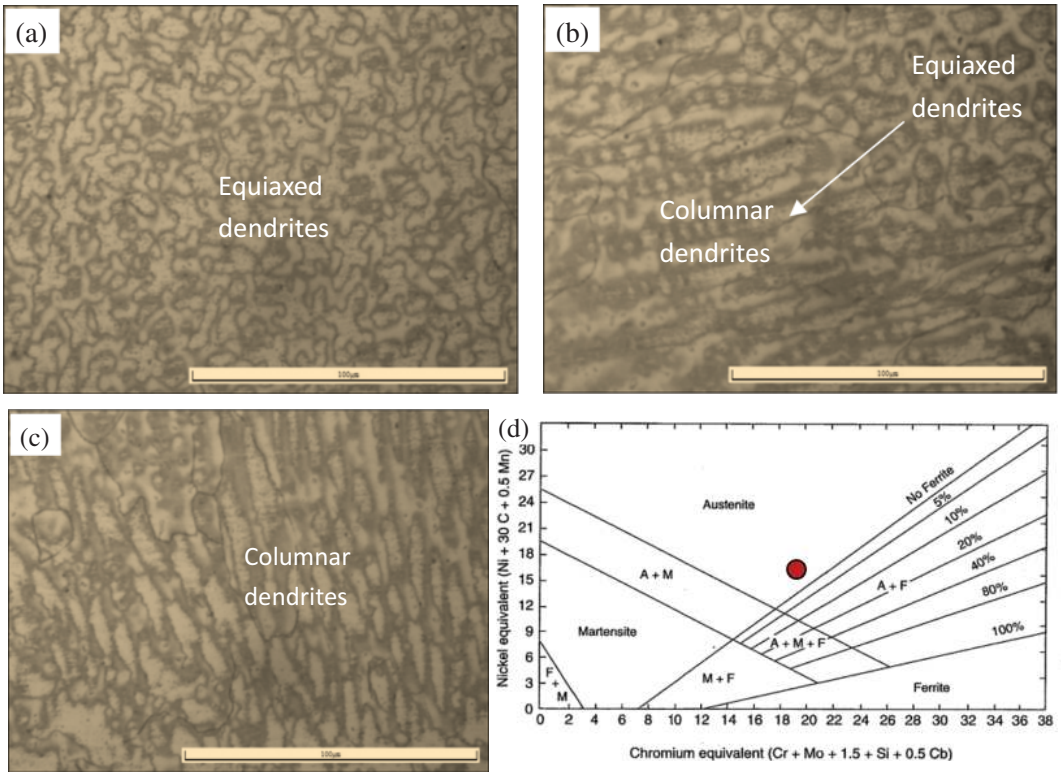

Figure 3: Microstructures of the weld metal (a) equiaxed dendrites with a grain size of 10 μm, (b) mixture of equiaxed dendrites and columnar dendrites, (c) columnar dendrites, (d) Schaeffer diagram.

the high nickel content promoted the stability of the austenite phase.

$$Cr_{eq} = Cr + Mo + 1.5Si + 0.5Nb = 19.78\% \quad (1)$$

$$Ni_{eq} = Ni + 30C + 0.5Mn = 20.33\% \quad (2)$$

Figure 3 shows the typical weld microstructures, consisting of austenitic grains, equiaxed dendrites and columnar dendrites. The transformation from equiaxed dendrites to columnar dendrites was due to the decreased G/R ratio [30]. Moreover, the nucleation and growth of equiaxed dendrites hindered columnar dendrite growth.

Interfacial microstructures

Figure 4 shows microstructures of the fusion line including T92 with weld metal and Super 304H with weld metal. As shown in Figure 4(a), the fusion line between T92 and weld metal was clear. The HAZ of T92 near the weld metal contains CG and fine-grain tempered martensites.

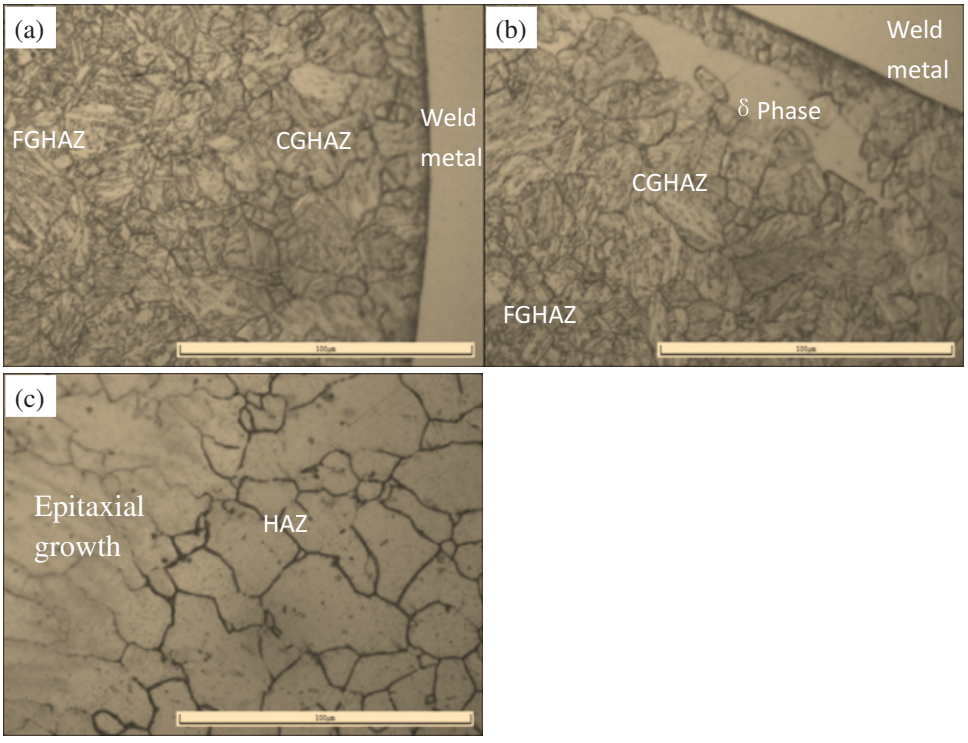

Figure 4: Microstructures of the fusion lines (a) between T92 and weld metal, (b) between T92 and weld metal, and (c) between Super 304H and weld metal.

The average grain sizes of the CGHAZ and the fine-grain HAZ were 25 μm and 10 μm, respectively. The formation of the CGHAZ was caused by the higher temperature during welding because the growth of grains was controlled by temperature and diffusion rate of atoms. Delta ferrites can be observed in the CGHAZ near the fusion line in Figure 4 (b). Delta ferrites are responsible for the fracture position of the CGHAZ in the weld joints owing to their detrimental effect on the mechanical properties of steels [28].

Figure 4(c) shows the fusion line between weld metal and Super 304H. The grains in the Super 304H HAZ were larger than those of the base metal, indicating that there was only grain growth during welding process. Furthermore, epitaxial growth was identified at the fusion line of Super 304H and weld metal.

Mechanical properties

Figure 5 shows the measured tensile strength of T92/Super 304H dissimilar weld joints with different groove angles. The tensile strength increased with increasing groove angle from 7° to 25°, all of which are above ASME standards for T92 and Super 304H. In addition, the fracture of the weld joints was located in the T92 HAZ, indicating tensile strength of the T92 HAZ was relatively weak. From the fracture morphology in Figure 5(b), it was found that the fracture mode was ductile fracture, owing to the high tensile strength. The alloy compositions of 18Cr-8Ni in Super 304H are significantly higher than those in T92. Based on the strengthening mechanism of nano-Cu phases and solution strengthening, the design and application strengths are higher in Super 304H than in T92. The contents of Ni and Cr in the weld metal are very high despite dilution during the welding process. Under solution strengthening of those alloys, the tensile strength of the weld metal exceeds that of T92. The T92 HAZ was subjected to high temperatures during welding, and the growth and aggregation of second-phase particles led to the relatively low tensile strength of the T92 HAZ.

Figure 6 shows the results of the microhardness tests. The hardness of the T92 HAZ with 7° groove angle was higher than that for other angles. The hardness values for the T92 HAZ were the highest among all the regions, whereas the lowest hardness values were obtained at the weld metal of the weld joints. When the groove angles were 15°, 20° and 25°, the hardness values were similar at respective positions on the joints. The highest hardness values were in the range of 310–325 at the T92

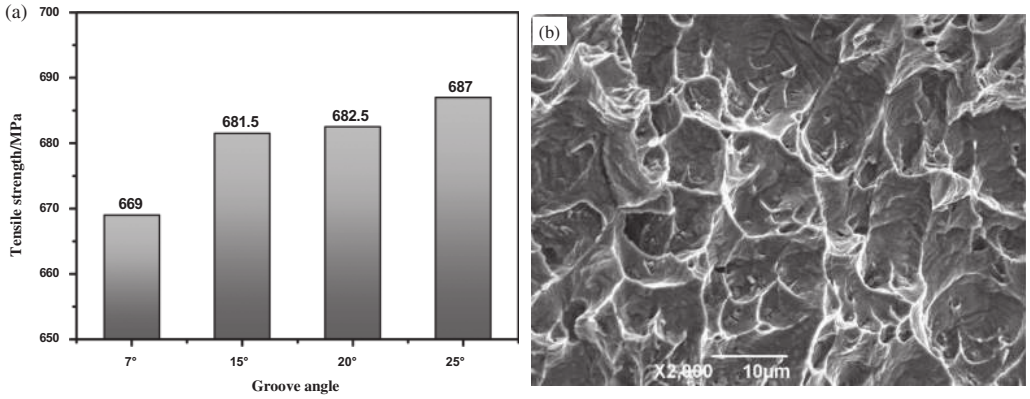

Figure 5: T92/Super 304H dissimilar weld joints (a) tensile test and (b) fracture morphology.

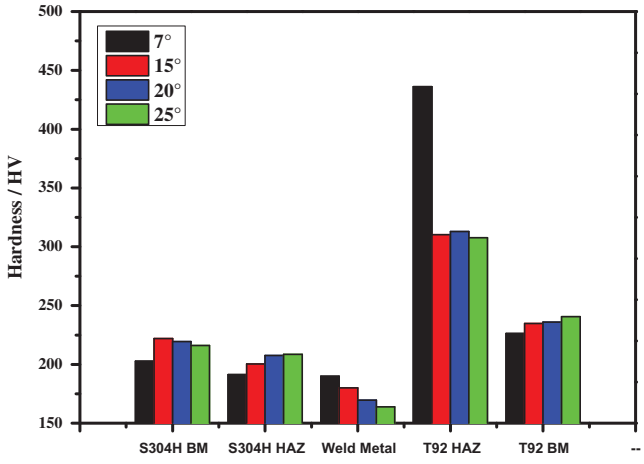

Figure 6: Microhardness of T92/Super 304H dissimilar weld joints.

HAZ, which was higher than the hardness value of the T92 base metal. This was caused by the transformation from austenitic to martensitic during the welding process. In contrast, the values in the Super 304H HAZ remain the same as the base metal because there was no phase transformation in the welding process.

The results of the bending tests are listed in Table 3. Half of the specimens welded with 7° groove angle failed during bending tests, indicating that the specimens were sensitive to solidification cracking. The cracks were 1.5 mm × 1 mm and 1.8 mm × 1 mm. Other specimens passed the bending test.

Table 3: Results of the bending test of T92/Super 304H dissimilar weld joints.

Groove angle	7°	15°	20°	25°
Qualified rate	50%	100%	100%	100%

Figure 7 shows the results of the X-ray inspection of the welded tubes. When the groove angles were 20° and 25°, the X-ray results met the standard. However, there were welding tube partial failures with the 7°, 10°, and 15° groove angles. For groove angles less than 15°, there were defects in the dissimilar weld joints.

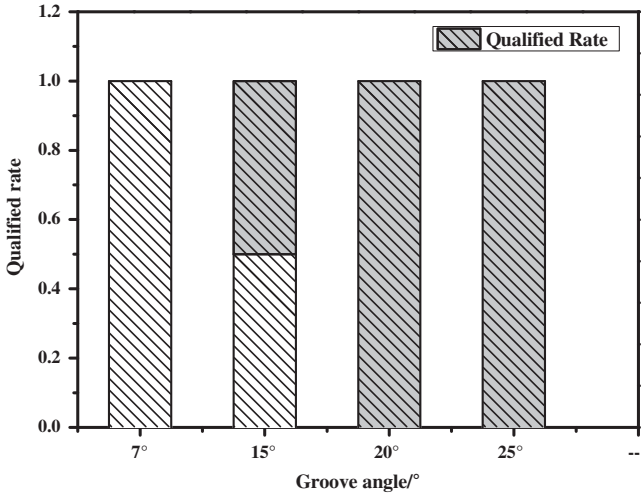

Figure 7: Results of the X-ray inspection of the welded tubes.

PWHT

Table 4 shows influence of PWHT on the mechanical properties of dissimilar weld joints. All specimens without PWHT failed during bending tests. The tensile strength of specimens after PWHT was higher than for those without PWHT. The phase of the T92 HAZ was partly transformed from martensite to sorbite. PWHT improved the microstructures of the weld joints especially for the T92 HAZ. Therefore its ductility and durability

Table 4: Results of the tensile and bending tests of T92/Super 304H dissimilar weld joints with and without post-weld heat treatment (PWHT).

State	R_m/MPa	Bending test
NO PWHT	530	Failed
	616	Failed
PWHT	676	Qualified
	689	Qualified

increased. Moreover, the residual stress was induced during welding process. Therefore, the mechanical properties of specimens after PWHT were better than those of specimens without PWHT.

Conclusions

1. PWHT enhances the mechanical properties of T92/Super 304H dissimilar steel weld joints.
2. Detrimental delta ferrites were found near the fusion line between the T92 base metal and the weld metal. Transformation from equiaxed dendrites to columnar dendrites was observed in the weld metal. Epitaxial growth was observed at the fusion line between the Super 304H base metal and the weld metal.
3. All of the fracture positions of T92/Super 304H weld joints were in the T92 HAZ. The tensile strength of weld joints increased slowly with increasing groove angle. The highest hardness among the weld joints was located in the T92 HAZ; the lowest was in the weld metal. The optimal groove angle for T92/Super 304H dissimilar steel weld joints is 20°.

References

[1] S. Missori and C. Koerber, Weld. J., 76 (1997) 125–134.
[2] A. Celik and A. Alsaran, Mater. Charact., 43 (1999) 311–318.
[3] X. Qi and X. Tian, Metal Hotworking Tech, 11 (2007) 008.
[4] P.J. Ennis, A. Zielinska-Lipiec, O. Wachter and A. Czyrska-Filemonowicz, Acta Mater., 45 (1997) 4901–4907.
[5] K. Kimura, K. Sawada and H. Kushima, Int. J. Mater. Res., 99 (2008) 395–401.
[6] K. Sawada, K. Kubo and F. Abe, Mater. Sci. Eng., A, 319 (2001) 784–787.
[7] F. Abe, Sci. Technol. Adv. Mater., 9 (2008) 013002.
[8] F. Abe, T. Horiuchi, M. Taneike and K. Sawada, Mater. Sci. Eng., A, 378 (2004) 299–303.
[9] V. Sklenička, K. Kuchařová, M. Svoboda, L. Kloc, J. Buršı and A. Kroupa, Mater. Charact., 51 (2003) 35–48.
[10] J. Jiang and L. Zhu, Mater. Sci. Eng., A, 539 (2012) 170–176.
[11] A. Di Schino, J.M. Kenny, M.G. Mecozzi and M.J. Barteri, Mater. Sci., 35 (2000) 4803–4808.
[12] A. Iseda, H. Okada, H. Semba and M. Igarashi, Energy Mater., 2 (2007) 199–206.
[13] T. Sourmail, Mater. Sci. Technol., 17 (2001) 1–14.
[14] J. Cao, Y. Gong, K. Zhu, Z.G. Yang, X.M. Luo and F.M. Gu, Mater. Des., 32 (2011) 2763–2770.
[15] Y.I. Gong, J. Cao, L.I.N.A. Ji, C. Yang and C. Yao, Fatigue Fract. Eng. Mater. Struct., 34 (2011) 83–96.
[16] G. Chen, Q. Zhang, J. Liu, J. Wang, X. Yu, J. Hua and X. Bai, Mater. Des., 44 (2013) 469–475.
[17] L. Falat, M. Svoboda, A. Výrostková and I. Petryshynets, Mater. Charact., 73 (2012) 15–23.
[18] R. Dehmolaei, M. Shamanian and A. Kermanpur, Mater. Charact., 59 (2008) 1447–1454.
[19] I. Hajiannia, M. Shamanian and M. Kasiri, Mater. Des., 50 (2013) 566–573.
[20] T.Y. Kuo and H.T. Lee, Mater. Sci. Eng., A, 338 (2002) 202–212.
[21] J. Cao, Y. Gong, Z.G. Yang, X.M. Luo and F.M. Gu, Int. J. Pressure Vessels Piping, 88 (2011) 94–98.
[22] A. Výrostková, V. Homolová, J. Pecha and M. Svoboda, Mater. Sci. Eng., A, 480 (2008) 289–298.
[23] L. Falat, A. Výrostková, V. Homolová and M. Svoboda, Eng. Failure Anal., 16 (2009) 2114–2120.
[24] T.W. Nelson, J.C. Lippold and M.J. Mills, Weld. J., 78 (1999) 329–337.
[25] T.W. Nelson, J.C. Lippold and M.J. Mills, Weld. J., 79 (2000) 267s-277s.
[26] H. Shah Hosseini, M. Shamanian and A. Kermanpur, Mater. Charact., 62 (2011) 425–431.
[27] J.N. DuPont, Int. Mater. Rev., 57 (2012) 208–234.
[28] J. Oñoro, Int. J. Pressure Vessels Piping, 83 (2006) 540–545.
[29] S. Kou, Welding Metallurgy, USA, Wiley (2002).
[30] J.C. Lippold and D.J. Kotecki, Mater. Charact., 55 (2005) 376.